Composition and temperature dependence of the Yb valence in $YbMn_6Ge_{6-x}Sn_x$ studied by RIXS

T. Mazet,[1,*] D. Malterre,[1] M. François,[1] L. Eichenberger,[1] M. Grioni,[2] C. Dallera,[3] and G. Monaco[4]

[1]*Institut Jean Lamour, UMR 7198, Université de Lorraine - B.P. 70239 54506 Vandœuvre-lès-Nancy, France*

[2]*Institute of Condensed Matter Physics, Ecole Polytechnique Fédérale de Lausanne (EPFL), 1015 Lausanne, Switzerland*

[3]*INFM-Dipartimento di Fisica, Politecnico di Milano, Piazza Leonardo da Vinci 32, 20133 Milano, Italy*

[4]*Physics Department, University of Trento, 38123 Provo, Trento, Italy*

(Received 3 June 2015; published 5 August 2015)

We investigate the composition and temperature (10–450 K) dependence of the Yb valence in $YbMn_6Ge_{6-x}Sn_x$ ($x = 0.0$, 3.8, 4.2, 4.4, and 5.5) using resonant inelastic x-ray scattering (RIXS). The observed change in the Yb valence with composition (from $\upsilon \sim 3$ for $x = 0$ to $\upsilon \sim 2.7$ for $x = 5.5$) is likely driven by negative chemical pressure effects due to the Sn for Ge substitution. While Yb is nonmagnetic in $YbMn_6Ge_{0.5}Sn_{5.5}$, intermediate valent Yb magnetically orders at unexpectedly high temperature (up to 90 K) in the alloys with $x = 3.8$, 4.2, and 4.4. The three latter alloys further exhibit an increase in the Yb valence upon cooling, which is opposite to the usual behavior. Interactions with the magnetically ordered Mn sublattice are invoked to account for these unprecedented phenomena through a simplified model based on an Anderson Hamiltonian with a Zeeman term mimicking the Mn-Yb exchange interactions. We further show that the Yb magnetic behavior in this series can be interpreted based on Doniach's picture. Compared with standard intermediate valent materials where Yb is embedded in a nonmagnetic matrix, the strong Mn-Yb exchange interaction enhances the intermediate valent Yb magnetic ordering temperature and allows for extending the stability domain of the Yb magnetic order towards lower Yb valence.

DOI: 10.1103/PhysRevB.92.075105 PACS number(s): 78.70.En, 71.28.+d, 75.30.Mb, 74.62.Bf

I. INTRODUCTION

Explaining the existence of atomic magnetic moments in metallic systems, including that of intermediate valent Yb, is an old and famous problem of condensed matter physics [1–5]. Yb, Ce, or U based metallic solids may present a wealth of fascinating behaviors (Kondo effect, intermediate valence, heavy fermion, nonconventional superconductivity, quantum criticality, etc.) as a result of the interplay between very large intra-atomic Coulomb interactions in the f shell and a partial delocalization due to hybridization of f states with conduction electrons [6]. These exotic phenomena may be tuned through a control parameter such as composition, pressure, or magnetic field. In the case of Yb, the energetically close $4f^{14}$ (Yb^{2+}) and $4f^{13}$ (Yb^{3+}) configurations are involved. The increase of the hybridization tends to favor the divalent state of larger atomic radius. While the divalent $4f^{14}$ state is nonmagnetic ($J = 0$), the trivalent $4f^{13}$ configuration is magnetic ($J = 7/2$). In intermediate valent Yb systems, the Kondo effect generally yields a screened moment with the formation of a nonmagnetic Fermi liquid ground state. However, in a rare few cases, intermediate valence is found to survive along with the stabilization of a magnetic order [7–10].

The interplay of magnetism and intermediate valence in Yb based metallic materials remains an open question. Until recently, the rare known situations of magnetic ordering of intermediate valent Yb were restricted to low temperature and to Yb valence close to $\upsilon \sim 3$ [7–9]. In materials where Yb is embedded in a nonmagnetic matrix, there is a competition between the Kondo effect and the RKKY-type magnetic interactions illustrated by the well-known Doniach's magnetic phase diagram [4,11]. For large hybridization between the f states and conduction electrons, the Kondo screening dominates whereas for low hybridization strength the magnetic ordering prevails. Quantum criticality and the breakdown of the Fermi-liquid behavior are expected near the magnetic instability (i.e., for intermediate hybridization) [12–14]. Up to now, materials with coexisting intermediate valent Yb and magnetic $3d$ sublattice have been scarcely investigated [15,16].

In a former paper [17], we discussed the high temperature magnetic ordering (up to 90 K) of intermediate valent Yb ($2.90 \leqslant \upsilon \leqslant 2.95$) in the $YbMn_6Ge_{6-x}Sn_x$ alloys with $x = 4.2$ and 4.4. This unprecedented high magnetic ordering temperature of intermediate valent Yb is very likely related to the strong $3d$ Mn–$5d$ Yb exchange interaction [18] and to the nonzero exchange field at the Yb site generated by the magnetic Mn sublattice.

The $YbMn_6Ge_{6-x}Sn_x$ series ($0 \leqslant x \leqslant 6$) comprises three solid solutions ($0 \leqslant x \leqslant 1.1$, $3.2 \leqslant x \leqslant 4.6$, and $5.3 \leqslant x \leqslant 6.0$) and two miscibility gaps [19]. All these alloys crystallize in the hexagonal ($P6/mmm$) $HfFe_6Ge_6$-type structure except the ternary stannide ($x = 6.0$) which adopts a slightly disordered variant [20,21]. The $HfFe_6Ge_6$ type of structure comprises one Mn site in $6i$ position, one Yb site ($1b$ position), and three metalloïd sites ($2c$, $2d$, and $2e$ positions). The structure can be viewed as an alternative stacking of two kinds of slabs along the c axis: the Mn-Yb,2d-Mn slab and the Mn-2e-2c-2e-Mn one. In $YbMn_6Ge_{6-x}Sn_x$, the Mn sublattice magnetically orders at or above room temperature and, depending on composition and temperature, exhibits various kinds of magnetic arrangements (ferromagnetic, helimagnetic, or antiferromagnetic) with an atomic Mn moment $m_{Mn} \sim 2.2\mu_B$. Magnetic ordering of the Yb sublattice is observed only for $x \leqslant 4.6$ (i.e., within the Ge-rich and intermediate solid solutions) at temperatures as high as 110 K. Besides the astonishingly high-magnetic ordering temperature of intermediate valent Yb in $YbMn_6Ge_{1.8}Sn_{4.2}$ and $YbMn_6Ge_{1.6}Sn_{4.4}$, our former study further evidenced an unusual increase in the Yb valence upon cooling [17]. In the present work, we

*thomas.mazet@univ-lorraine.fr

investigate the composition and temperature dependence of the Yb valence for the whole $YbMn_6Ge_{6-x}Sn_x$ series by resonant inelastic x-ray scattering (RIXS).

The organization of the paper is as follows. Section II provides the experimental details. The results are presented and analyzed in Sec. III before a discussion in Sec. IV and a short conclusion in Sec. V.

II. EXPERIMENTAL DETAILS

The powder $YbMn_6Ge_{6-x}Sn_x$ samples with $x = 0.0$, 3.8, 4.2, 4.4, and 5.5 were prepared from high-purity elements as described in Ref. [19]. The precise chemical composition of the alloys was checked by microprobe measurements using a CAMECA SX100. Long duration room-temperature x-ray diffraction patterns were collected using a Philips X'Pert Pro diffractometer ($\lambda = 1.54056$ Å) and refined with the Rietveld method using the FULLPROF software [22] to check the crystal structure of the compounds and the purity of the samples. All compounds were found to be isotypic with $HfFe_6Ge_6$ ($P6/mmm$), as expected. No attempt has been done to prepare and to study $YbMn_6Sn_6$ (i.e., $x = 6.0$), which is known to crystallize in a slightly less ordered variant [20,21]. The refinements also indicated that the two richer Ge samples ($x = 0.0$ and 3.5) contain a few wt. % of the ferromagnetic Mn_5Ge_3 impurity ($T_C \sim 300$ K), while the Yb_2O_3 level was found below 2 wt. % in all cases. The diffractometer was also used to record patterns in the 300–15 K temperature range which were analyzed in pattern matching mode to determine the temperature dependence of the lattice parameters. dc magnetization data were recorded using a Physical Property Measurement System (PPMS) from Quantum Design. The temperature variation of the magnetization was recorded upon cooling between 350 and 5 K in a field of 500 Oe. Hysteresis loops were recorded at 5 K in field up to 90 kOe.

The partial fluorescence yield x-ray absorption spectroscopy (PFY XAS) and resonant inelastic x-ray scattering (RIXS) measurements were carried out at beamline ID16 of the European Synchrotron Radiation Facility (Grenoble, France). The beamline was equipped with a fixed-exit Si(111) monochromator and a toroidal Rh-coated focusing mirror providing a 130×50 μm^2 (H × V) beam spot at the sample position. The experiment was performed in reflection geometry. The emitted radiation was energy-analyzed using a Rowland circle spectrometer based on a 1-m radius, spherically bent Si(620) crystal, and a Si avalanche photodiode detector. The scattering plane was horizontal, i.e., parallel to the linear polarization vector of the incident beam. The spectra were collected at scattering angle $2\theta = 90°$ to minimize the nonresonant scattering contribution. The total energy resolution was ~1.7 eV. Freshly scraped samples in the form of pressed pellets were mounted in a He cryostat and measured in high (10^{-8} mbar) vacuum in the 300–10 K temperature range. The alloys with $x = 4.2$ and 4.4 were further investigated up to 450 K in an oven.

III. EXPERIMENTAL RESULTS

The RIXS and PFY XAS spectra recorded at 300 K for the five studied compounds are shown in Figs. 1(a) and 1(b),

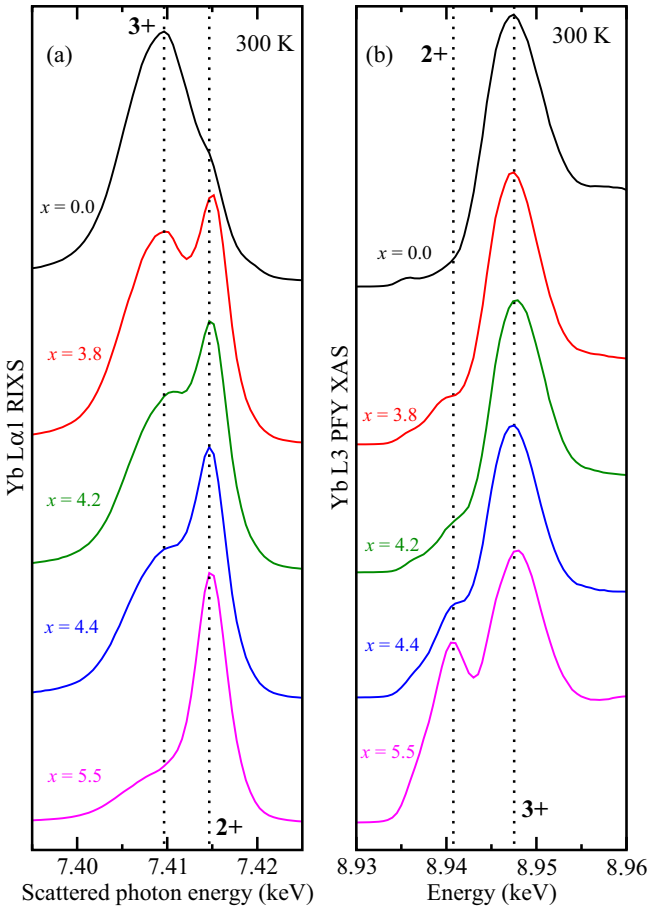

FIG. 1. (Color online) Room-temperature RIXS (a) and PFY XAS (b) spectra for the alloys with $x = 0.0$, 3.8, 4.2, 4.4, and 5.5.

respectively. The RIXS spectroscopy couples the initial state with $3d^9 4f^{13}$ and $3d^9 4f^{14}$ final states [23–25]. The weak Yb^{2+} contribution can be enhanced by tuning the incident photon energy to the energy of the Yb^{2+} edge in the L_3 PFY XAS. Due to the resonant nature of RIXS, the Yb valence cannot be obtained from a simple ratio of the Yb^{2+} and Yb^{3+} intensities. Then following a procedure previously proposed [23], we have normalized the RIXS ratio of these two structures with the ratio obtained from the low temperature L_3 PFY XAS data. Figure 1 evidences a strong valence change with composition. As the Sn content increases from $x = 0.0$ to $x = 5.5$, a marked spectral weight transfer from the "3+" component towards the "2+" one occurs.

The variation of the room-temperature Yb valence with Sn content is shown in Fig. 2(b) together with that of the cell volume [Fig. 2(a)]. While Yb is basically trivalent in $YbMn_6Ge_6$, there is an increasing departure from trivalence upon increasing the Sn content throughout the series, but even in the richest Sn compound studied ($x = 5.5$), Yb is found far from divalence ($\upsilon \sim 2.72$). The concomitant increase in the cell volume and reduction in the Yb valence upon the Sn for Ge substitution strongly suggests that the driving mechanism responsible for the Yb valence change throughout the $YbMn_6Ge_{6-x}Sn_x$ series is a reduction of the chemical pressure, the increase in the interatomic distances favoring

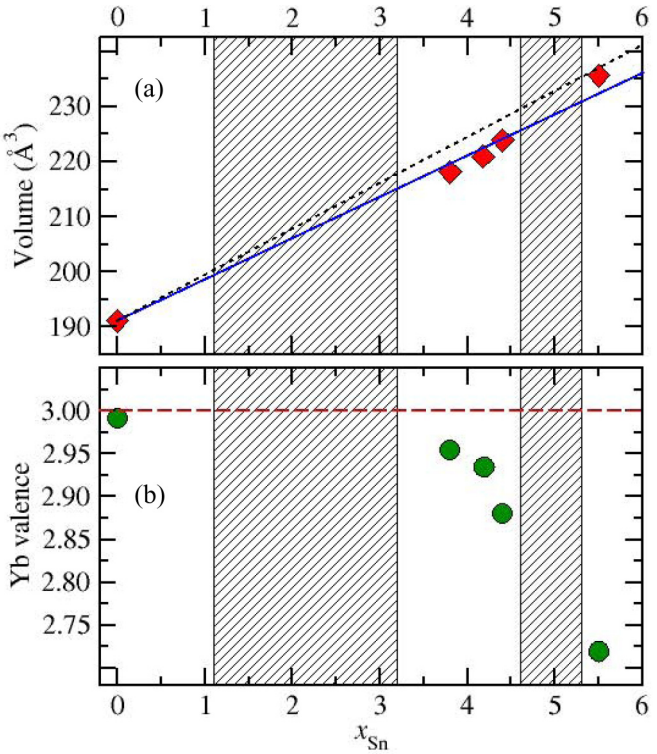

FIG. 2. (Color online) (a) Variation of the room-temperature cell volume with the Sn content. The continuous line marks volumes expected for a fully trivalent Yb: it joins the cell volume of $YbMn_6Ge_6$ with that of $LuMn_6Sn_6$ (data from Ref. [28]). The dotted line, which links the cell volume of $YbMn_6Ge_6$ with that of $YbMn_6Sn_6$ (data from Ref. [20]), corresponds to a simple linear variation of the cell parameters. (b) Variation of the room-temperature Yb valence with the Sn content. The shaded areas mark the miscibility gaps [19].

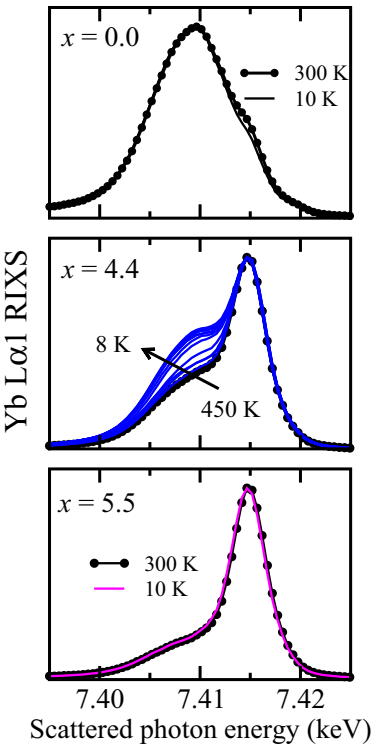

FIG. 3. (Color online) RIXS spectra for $x = 0.0$ and 5.5 at 300 K and 10 K. RIXS spectra for $x = 4.4$ between 450 and 8 K.

divalent Yb of larger atomic radius than trivalent Yb (see, e.g., Ref. [9]). It cannot however be excluded that electronic modifications arising from the nature of the Sn $5p$ compared to Ge $4p$ wave function also interfere. For instance, the rise in T_C with Si content in the magnetocaloric $Gd_5(Si_xGe_{1-x})_4$ alloys has been shown to be mainly due to an electronic effect, while the volume effect only plays a secondary role [26].

There is no linear relation between cell volume and Yb valence which only weakly evolves for $0 \leqslant x < 3.8$ and then varies rapidly for higher Sn content [Fig. 2(b)]. This shows that in $YbMn_6Ge_{6-x}$ Sn_x the Yb valence is more sensitive to the Sn content for x around ~4. Since the driving mechanism is expected to be the lattice expansion, this suggests that in this Sn composition range the Yb valence strongly depends on interatomic distances. We also observe that only for $x = 5.5$ the cell volume is larger than that expected for a fully trivalent Yb. Estimating the Yb valence in solids from lattice constants may thus be somewhat misleading. This also appears for instance in Table I of Ref. [27]. We speculate that Yb is not fully divalent even in the ternary $YbMn_6Sn_6$, unless the Yb valence hugely varies in the Sn-rich $YbMn_6Ge_{6-x}Sn_x$ terminal solid solution.

The RIXS spectra obtained at 300 K and 10 K for $x = 0$ and 5.5 are shown in Fig. 3 together with the spectra recorded in the 8–450 K temperature range for $x = 4.4$. In both the Sn-rich $x = 5.5$ compound and the ternary germanide $YbMn_6Ge_6$, the RIXS spectra are insensitive to temperature variation whereas the 3+ component is found to increase upon cooling for the alloy with $x = 4.4$. Figure 4 shows the thermal variation of the Yb valence for the whole series. The Yb valence of the alloys with $x = 3.8$ and 4.2 is found to slightly rise when lowering temperature similarly to the behavior of $x = 4.4$. Except in $YbMn_6Ge_6$ where Yb is trivalent, all others alloys contain intermediate valent Yb over the whole investigated temperature range.

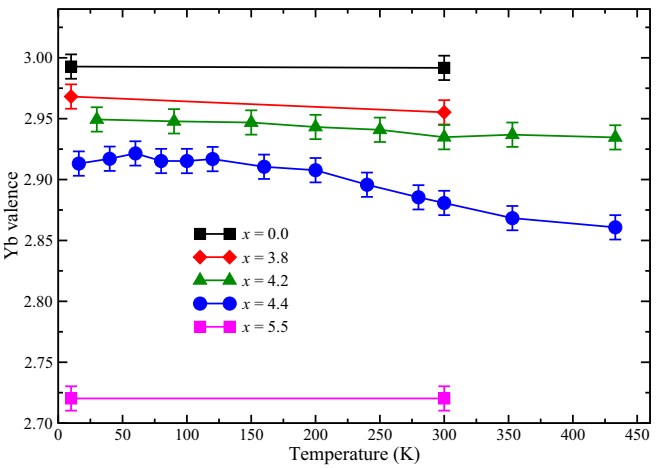

FIG. 4. (Color online) Thermal dependence of the Yb valence in $YbMn_6Ge_{6-x}$ Sn_x ($x = 0.0$, 3.8, 4.2, 4.4, and 5.5).

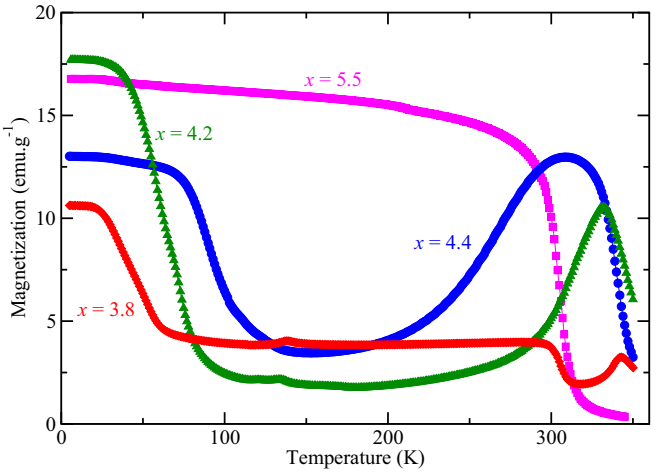

FIG. 5. (Color online) Thermal dependence of the magnetization of $YbMn_6Ge_{6-x}$ Sn_x ($x = 3.8$, 4.2, 4.4, and 5.5) in an applied field of 500 Oe. The weak ferromagnetic component seen on the curve of $x = 3.8$ below ~300 K is due to the magnetic ordering of the Mn_5Ge_3 impurity. The data for $x = 0.0$ are not shown: the Mn sublattice antiferromagnetically orders above 350 K (the highest temperature of the experiment) and the low-temperature behavior is overshadowed by the ferromagnetic Mn_5Ge_3 impurity.

In $YbMn_6Ge_{6-x}Sn_x$, the Mn sublattice magnetically orders at or above room temperature and shows a complex dependence on temperature and composition [19]. To summarize: in the Ge-rich alloys, the Mn sublattice is antiferromagnetic while upon increasing the Sn content a high temperature ferromagnetic state develops at the expense of the low temperature spiral arrangements. In the Sn-rich solid solution ($x \geqslant 5.3$), the Mn sublattice is purely ferromagnetic. From previous magnetization, neutron diffraction, and ^{170}Yb Mössbauer spectroscopy experiments, it has been shown that Yb does magnetically order at quite high temperature (up to 110 K) in $YbMn_6Ge_{6-x}Sn_x$ with $x \leqslant 4.6$ [19]. This manifests through the strong rise in the magnetization at low temperature on the thermomagnetic data we recorded on the present samples (Fig. 5). We identify the Yb ordering temperature (T_{Yb}) with the low-temperature minimum of $\frac{\partial M}{\partial T}$, and find $T_{Yb} \sim 40$ K, ~70 K, and ~90 K for $x = 3.8$, 4.2, and 4.4, respectively. Hence we can conclude that in the $YbMn_6Ge_{6-x}Sn_x$ alloys of the intermediate solid solution ($3.2 \leqslant x \leqslant 4.6$), intermediate valent Yb magnetically orders at quite high temperature, an unprecedented phenomenon that likely finds its origin in the interaction with the magnetic Mn sublattice. In $YbMn_6Ge_{0.5}Sn_{5.5}$, intermediate valent Yb does not order and the magnetic behavior is only related to the ferromagnetic Mn sublattice. Thus the magnetic ordering of intermediate valent Yb disappears for $2.7 < \upsilon < 2.9$. The Yb valence also influences the Mn magnetic behavior. Numerous previous studies have shown that lowering the R valence in RMn_6X_6 (X = Ge or Sn) or the average metalloid valence in pseudoternaries $RMn_6X_{6-x}X'_x$ (X' = In or Ga) favors the stabilization of a ferromagnetic Mn sublattice: the RMn_6X_6 compounds with trivalent R are antiferromagnets or helimagnets and only divalent R elements and/or partially substituted Ga or In alloys can bring the Mn sublattice to ferromagnetism (see Refs. [19,20,29–32]). This dependence on the R valence is conspicuous in $YbMn_6Ge_{6-x}Sn_x$: the ferromagnetic region just below the Mn ordering temperature enlarges progressively as the Yb valence decreases throughout the series. In $YbMn_6Ge_{0.5}Sn_{5.5}$, the Yb valence is low enough for the Mn sublattice to be ferromagnetic over the whole ordered temperature range.

The Yb valence may change with temperature. Increasing the temperature usually yields an increase in the Yb valence as described in the single impurity Anderson model [33]. The energy spectrum is characterized by a singlet intermediate valent ground state and a manifold of purely trivalent excited states (at an excitation energy $\delta = k_B T_K$). At low temperature ($T \ll T_K$) the Yb valence is determined by the valence admixture in the ground state and increases with temperature due to the thermal population of the trivalent excited states. However, this picture does not describe the temperature dependence of the valence in the $3.8 \leqslant x \leqslant 4.4$ composition range since a valence increase is observed upon cooling (Fig. 4). To explain this anomalous temperature dependence and the unusual Yb magnetic behavior in the $YbMn_6Ge_{6-x}Sn_x$ alloys, we have proposed a toy model in Ref. [17] where the system is simply represented by one $S = 1/2$ impurity state with energy $\varepsilon_i < 0$ and Coulomb interactions (U) for Yb atoms hybridized (V) with an infinitely narrow band at energy $\varepsilon_0 = 0$ corresponding to the itinerant electron gas. Moreover, magnetic interactions are modeled by a Zeeman interaction so that the Hamiltonian can be written

$$H = \sum_\sigma \varepsilon_i n_{i,\sigma} + \varepsilon_0 \sum_\sigma n_{0,\sigma} + V \sum_\sigma (a^\dagger_{i,\sigma} a_{0,\sigma} + \text{c.c.}) + U n_{i,\sigma} n_{i,-\sigma} + g_i \mu_B \sigma_{i,z} B. \quad (1)$$

The last term is a Zeeman Hamiltonian on the localized impurity electron [34] (not on the itinerant one), whereas the other ones represent an Anderson-like Hamiltonian. In the infinite U limit, the double occupancy of the impurity orbital (corresponding to two holes in the $4f$ shell of Yb and then to the $4f^{12}$ configuration) is forbidden and the basis states are $|0\rangle$ for the unoccupied impurity state (corresponding to the filled $4f$ shell and then to the $4f^{14}$ configuration) and the $|\eta,\eta'\rangle$ with $\eta,\eta' = \uparrow$ or $\downarrow$ for respectively the spin of the impurity and itinerant electrons (corresponding to the $4f^{13}$ configuration). Without the Zeeman term, the ground state is a nonmagnetic Kondo-like singlet

$$|\Psi\rangle = c_0|0\rangle + c_1 \frac{|\uparrow\downarrow\rangle - |\downarrow\uparrow\rangle}{\sqrt{2}}$$

at $\varepsilon_i - \delta$, whereas the excited states correspond to the triplet ($S = 1$) states at ε_i and a high energy singlet state corresponding mainly to the nonoccupied impurity state. An increase of the hybridization parameter V leads to an increase in $|c_0|$ (decrease of the valence) and δ. A finite magnetic field changes the ground state and leads to the appearance of a magnetic moment associated with the impurity state. In the high field limit, the impurity state is fully polarized and the ground state is the doublet $|\uparrow\uparrow\rangle, |\uparrow\downarrow\rangle$. In Ref. [17], we showed the field dependence of the impurity valence ($\upsilon = 2 + |c_1|^2$) and of the localized magnetic moment. The increase in the magnetic field leads to a crossover from a nonmagnetic state to

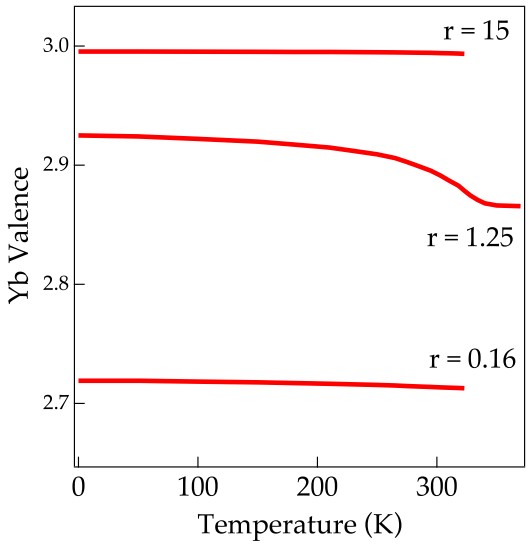

FIG. 6. (Color online) Calculated temperature dependence of the Yb valence obtained for several $r = \mu_B B/\delta$ parameters. The $r \gg 1$ corresponds to the $x = 0$ sample ($\upsilon \sim 3$), whereas the Yb valence in the $x = 4.4$ and 5.5 alloys can be described with $r = 1.25$ and $r = 0.15$, respectively.

a completely polarized magnetic state and is in agreement with more elaborate calculations [35,36]. With such a very crude model, we were able to reproduce the anomalous temperature dependence of the Yb valence (in the $x = 4.2$ and $x = 4.4$ samples) with a temperature dependence of the Zeeman term $[B(T)]$ resulting from the magnetization of the Mn lattice. A similar increase in the Yb valence upon increasing the external magnetic field has been observed in $YbAgCu_4$ [37].

In Fig. 6, we present the temperature dependence of the Yb valence obtained from our simple approach for different cases. The key parameter is the ratio $r = \mu_B B(0)/\delta$ comparing the energy stabilization of the nonmagnetic singlet state due to hybridization and the Zeeman energy. The qualitative evolution of r can be understood from the composition dependence of the Yb valence. Indeed, for $x = 0$, the valence is close to 3, corresponding to a very small Kondo energy and then a large r parameter. In this limit, the valence remains very close to 3 for the whole temperature range. The Kondo energy scale increases with increasing valence admixture leading to a decrease of the r parameter. The anomalous temperature dependence of the $x = 4.4$ alloy is reproduced with comparable characteristic energies ($r = 1.25$). For the $x = 5.5$ alloy, the large valence admixture associated with the nonmagnetic Yb sublattice suggests that the hybridization energy is larger than both the Zeeman energy and the thermal energy ($k_B T$). In this limit, the Yb valence is expected to be independent of the Mn magnetization and then independent of temperature. Our calculation reported in Fig. 6 confirms that the Yb valence in this limit is nearly temperature independent. Comparison with Fig. 4 shows that this crude model is able to qualitatively reproduce the Yb valence and its temperature dependence in this series.

The temperature dependence of the reduced cell volume of the five compounds studied is shown in Fig. 7. All the alloys present the usual lattice contraction upon cooling. The

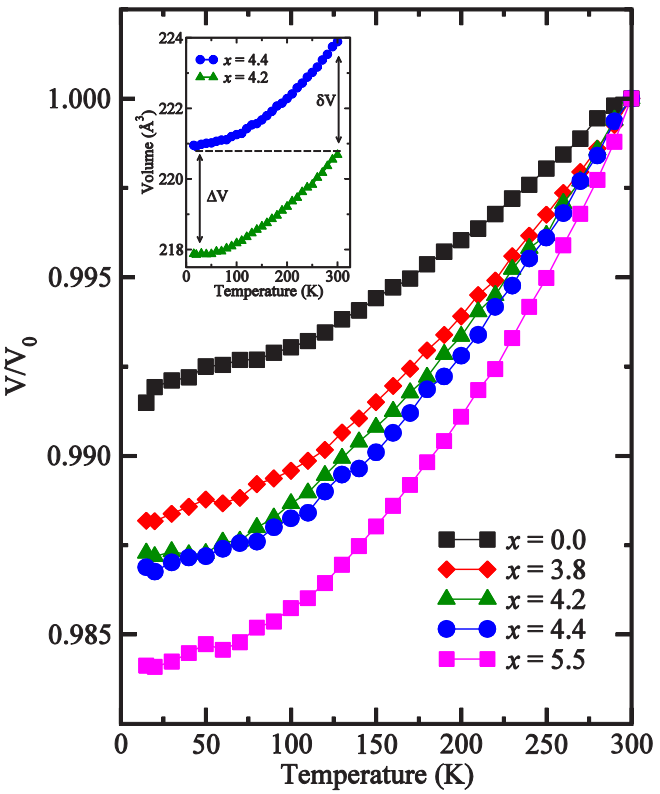

FIG. 7. (Color online) Thermal dependence of the reduced volume V/V_0 (V_0 is the room-temperature volume) of $YbMn_6Ge_{6-x}Sn_x$ ($x = 3.8$, 4.2, 4.4, and 5.5) between 300 K and 10 K. The inset shows the thermal variation of the cell volume for $x = 4.2$ and 4.4.

slight thermal variation of the Yb valence in the alloys with $x = 3.8$, 4.2, and 4.4 does not yield an observable anomaly. The enhancement of the thermal variation of the cell volume upon increasing x originates from a weakening of the chemical bonds. In such kind of intermetallics, the bonds with Sn are weaker than those with Ge [32,38]. In addition, the reduction of the Yb valence leads to less $5d$ valence electrons which further contributes to weaken the related interatomic bondings. Weaker chemical bonds yield a less steep Morse's potential and thus a wider thermal variation.

We further note (inset of Fig. 7) that the lattice contraction from $x = 4.4$ to $x = 4.2$ ($\delta V/V \sim -1.4\%$ at 300 K) is similar to the thermal contraction ($\Delta V/V_0 \sim -1.3\%$ for $x = 4.2$ and 4.4, where V_0 is the cell volume at 300 K) and that the observed Yb valence increase due to composition change ($\Delta\upsilon \sim +0.05$) is close to that measured upon cooling ($\Delta\upsilon \sim +0.02$ and $+0.03$ for $x = 4.2$ and 4.4, respectively). Therefore, we propose that, owing to the apparent strong sensitivity of the Yb valence to interatomic distances in this composition range, the lattice contraction might play a role in the observed anomalous thermal variation of the Yb valence in addition to the model we proposed above.

IV. DISCUSSION

In $YbMn_6Ge_{6-x}Sn_x$, the Yb valence decreases upon increasing the Sn content, most likely because of negative chemical pressure effects associated with the replacement of

Ge atoms by larger Sn atoms. The dependence of the Yb valence on the Sn content is more pronounced for $x \sim 4.0$, which suggests that the Yb valence could be more sensitive to lattice variation in the vicinity of this composition range. Experiments under external pressure on intermediate valent Yb materials [16,27,39,40] often yield a nonlinear variation of the Yb valence, suggesting again that for a certain material-dependent hybridization range the Yb valence is more sensitive to (external or chemical) pressure variation (i.e., to lattice constant change). We propose that in the $YbMn_6Ge_{6-x}Sn_x$ alloys with $x \sim 4.0$, the electronic structure would be such that the Yb valence strongly depends on interatomic distances. Though Yb is already in the intermediate valence regime within the alloys with $x = 4.2$ and 4.4 ($\upsilon \sim 2.9$), their cell volume does not depart from that expected for a fully trivalent Yb and only the alloy with $x = 5.5$ ($\upsilon \sim 2.7$) has *abnormally* large lattice constants.

Except for the ternary germanide $YbMn_6Ge_6$ within which Yb is basically trivalent, Yb was found in intermediate valent state over the whole investigated temperature range in all studied alloys. Accordingly, unlike the common belief, we showed that the high temperature magnetic order of the Yb sublattice in the alloys with $x = 3.8$, 4.2, and 4.4 ($T_{Yb} \sim 40$ K, 70 K, and 90 K, respectively) involves intermediate valent Yb. This likely results from the strong exchange field produced by the Mn sublattice at the Yb site, a situation that had never been observed before. The thermal variation of the Yb valence is another striking feature of $YbMn_6Ge_{6-x}Sn_x$ in the intermediate solid solution. While the Yb valence of the alloys with $x = 0.0$ and 5.5 does not change with temperature, that of the magnetic intermediate valent Yb alloys ($x = 3.8$, 4.2, and 4.4) increases upon cooling, at odds to the usual behavior. We were able to explain both the occurrence of magnetic intermediate valent Yb and the anomalous temperature dependence of the Yb valence thanks to a simple model based on an Anderson Hamiltonian including a Zeeman term to account for the Mn-Yb exchange interactions. Because of the presumed sensitivity of the alloys near $x \sim 4$ to changes of the interatomic distances, we also suggested that the lattice contraction might play a role in the unusual thermal variation of the Yb valence.

Figure 8 shows the composition dependence of the Yb ordering temperature (data from the present work and from Ref. [19]) and Yb magnetic moment (data from Ref. [19]). Weak changes of the Yb valence induced by subtle chemical composition variation in the intermediate solid solution are seen to yield drastic modifications in the Yb moment and Yb ordering temperature. The inspection of Fig. 2 and Fig. 8 leads to an *a priori* puzzling finding: the Sn for Ge substitution, resulting in an increase of the $4f$-conduction electrons hybridization strength (i.e., a lowering of the Yb valence), causes an enlargement of the cell volume, a decrease in the Yb moment, but a sharp increase of the Yb magnetic ordering temperature. The reduction in the Yb moment is very likely a consequence of the enhancement of the Kondo screening. In this context, the concomitant increase in T_{Yb} though the interatomic distances increase may appear more difficult to understand. Actually, the simultaneous reduction of the Yb moment and rise of the ordering temperature upon increasing the hybridization is predicted by the Doniach's

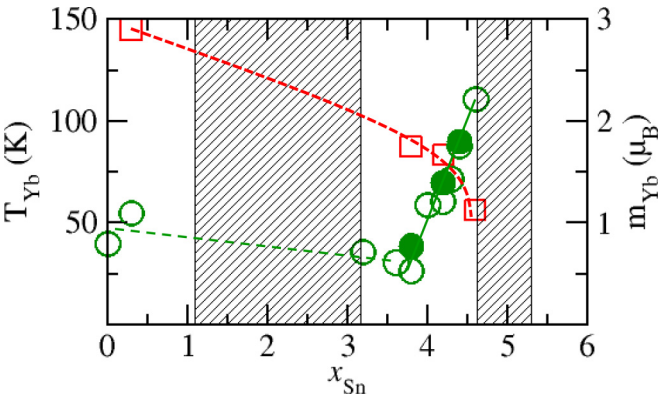

FIG. 8. (Color online) Composition dependence of the Yb ordering temperature (green circles, left scale) and Yb magnetic moment (red squares, right scale). Data in open symbols are taken from Ref. [19]. The lines are guides to the eye.

model in the low hybridization region. Similar behaviors were observed upon changing the external or chemical pressure in $CeRh_3B_2$ [11,41], another hybridized $4f$ material with unusually high magnetic ordering temperature of the $4f$ sublattice. In $YbMn_6Ge_{6-x}Sn_x$, the main novelty compared with standard intermediate valent Yb materials is the interaction with the magnetic Mn sublattice which has two effects on the magnetic phase diagram. It yields Yb magnetic ordering temperatures that are one or two order(s) of magnitude higher than those of previously identified intermediate valent Yb materials [7–9] and stabilizes the magnetic order for relatively low values of the Yb valence ($\upsilon \sim 2.9$).

The unique $YbMn_6Ge_{6-x}Sn_x$ alloys in the intermediate solid solution ($3.2 \leqslant x \leqslant 4.6$) offer therefore the possibility for investigating the magnetic behavior of intermediate valent Yb with a high degree of hybridization over a broad temperature interval. The hysteresis loops recorded at 5 K for $x = 5.5$ (nonmagnetic Yb, ferromagnetic Mn) and $x = 4.4$ (magnetic Yb forming a collinear ferrimagnetic structure with the ferromagnetic Mn sublattice) are compared in Fig. 9. It is seen that the presence of magnetic intermediate valent Yb ($x = 4.4$)

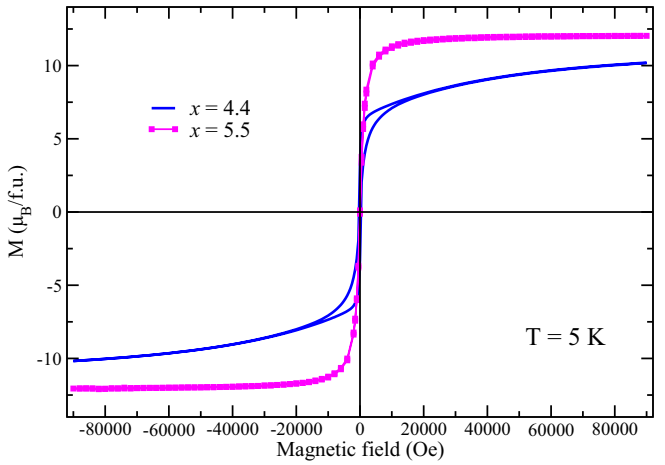

FIG. 9. (Color online) Hysteresis loops of $x = 4.4$ and $x = 5.5$ at 5 K in field up to 90 kOe.

leads to an opening of the loop with nonzero coercivity ($H_c \sim 300$ Oe) and remanence, while the alloy with $x = 5.5$ behaves as a soft ferromagnet. This strongly suggests that a significant orbital contribution to the intermediate valent Yb magnetic moment still persists, as expected from localized magnetism. On the other hand, it is known from band structure calculations that intermediate valent Yb implicates partially delocalized f electrons [42,43]. Owing to the relatively strong hybridized character of the Yb $4f$ states in the $YbMn_6Ge_{6-x}Sn_x$ alloys of the intermediate solid solution ($3.2 \leqslant x \leqslant 4.6$), it cannot be excluded that partially delocalized $4f$ electrons interfere in their astonishing magnetic behavior.

In $YbMn_6Ge_{6-x}Sn_x$, the Yb magnetic ordering is lost for $4.6 < x < 5.3$. As recalled in the Introduction, quantum criticality and non-Fermi-liquid behaviors can be observed in the vicinity of the magnetic instability [12–14]. It would therefore be interesting to investigate the physical behaviors of $YbMn_6Ge_{6-x}Sn_x$ close to the Yb magnetic instability. For that purpose, and also to clarify the role of the interatomic distances on the Yb valence in this series, various experiments under pressure are in progress. Pressure increase on initially nonmagnetic intermediate valent Yb solid can allow stabilizing Yb magnetic ordering and tuning the materials to a quantum phase transition [44,45].

V. CONCLUSION

We have investigated the composition and temperature dependence of the Yb valence in $YbMn_6Ge_{6-x}Sn_x$ ($x = 0.0$, 3.8, 4.2, 4.4, and 5.5) using RIXS spectroscopy in the 10–450 K temperature range. The Yb valence decreases upon increasing the Sn content (from $\upsilon \sim 3$ for $x = 0$ to $\upsilon \sim 2.7$ for $x = 5.5$), most likely because of chemical pressure effects. The $YbMn_6Ge_{6-x}Sn_x$ alloys with $3.2 \leqslant x \leqslant 4.6$ present the unique situation of a strongly magnetized $3d$ sublattice exerting a significant exchange field at the intermediate valent Yb site. This yields astonishingly high magnetic ordering temperatures for intermediate valent Yb (up to ~110 K) and shifts the Yb magnetic instability towards significantly lower valence ($2.7 < \upsilon < 2.9$) than in standard intermediate valent materials where Yb is alloyed with nonmagnetic elements (magnetic instability close to $\upsilon \sim 3$). In addition, the alloys of the intermediate solid solution ($3.2 \leqslant x \leqslant 4.6$) show an increase of the Yb valence upon cooling, opposite to the usual behavior, which we have also tentatively ascribed to the presence of a magnetized Mn sublattice with the possible supplementary participation of the lattice contraction. Further experimental and theoretical works are needed for a better understanding of the unusual Yb behavior in this series.

ACKNOWLEDGMENTS

We are indebted to the ESRF (Grenoble, France) for the provision of research facilities. Work at Lausanne was supported by the Swiss NSF.

[1] J. Friedel, J. Phys. Radium **19**, 573 (1958).
[2] P. W. Anderson, Phys. Rev. **124**, 41 (1961).
[3] M. B. Maple and D. Wohlleben, *Demagnetization of Rare Earth Ions in Metals Due to Valence Fluctuations*, AIP Conf. Proc. No. 18 (AIP, New York, 1974), p. 447.
[4] S. Doniach, Physica B+C **91**, 231 (1977).
[5] Y. Kuramoto, Z. Phys. B **40**, 293 (1981).
[6] For a review, see P. Coleman, in *Handbook of Magnetism and Avanced Magnetic Materials*, edited by H. Kronmüller and S. Parkin (Wiley, New York, 2007), and references therein.
[7] G. V. Eynatten, C. F. Wang, N. S. Dixon, L. S. Fritz, and S. S. Hanna, Z. Phys. B **51**, 37 (1983).
[8] F. Oster, B. Politt, E. Braun, H. Schmidt, J. Langen, and N. Lossau, J. Magn. Magn. Mater. **63-64**, 629 (1987).
[9] C. Klinger, C. Krellner, M. Brando, C. Geibel, F. Steglich, D. V. Vyalikh, K. Kummer, S. Danzenbächer, S. L. Molodtsov, C. Laubschat, T. Kinoshita, Y. Kato, and T. Muro, Phys. Rev. B **83**, 144405 (2011).
[10] D. Malterre, M. Grioni, P. Weibel, B. Dardel, and Y. Baer, Phys. Rev. B **48**, 10599 (1993).
[11] A. L. Cornelius and J. S. Schilling, Phys. Rev. B **49**, 3955 (1994), and references therein.
[12] H. v. Löhneysen, J. Magn. Magn. Mater. **200**, 532 (1999).
[13] H. v. Löhneysen, A. Rosch, M. Vojta, and P. Wölfe, Rev. Mod. Phys. **79**, 1015 (2007).
[14] M. C. Aronson, M. S. Kim, M. C. Bennett, Y. Janssen, D. A. Sokolov, and L. Wu, J. Low Temp. Phys. **161**, 98 (2010).
[15] M. Hofmann, S. J. Campbell, P. Link, S. Fiddy, and I. Goncharenko, Physica (Amsterdam) **385B-386B**, 330 (2006).
[16] H. Yamaoka *et al.*, Phys. Rev. Lett. **107**, 177203 (2011).
[17] T. Mazet, D. Malterre, M. François, C. Dallera, M. Grioni, and G. Monaco, Phys. Rev. Lett. **111**, 096402 (2013).
[18] M. S. S. Brooks, L. Nordström, and B. Johansson, J. Phys.: Condens. Matter **3**, 2357 (1991).
[19] T. Mazet, H. Ihou-Mouko, D. H. Ryan, C. J. Voyer, J. M. Cadogan, and B. Malaman, J. Phys.: Condens. Matter **22**, 116005 (2010).
[20] T. Mazet, R. Welter, and B. Malaman, J. Magn. Magn. Mater. **204**, 11 (1999).
[21] S.-Q. Xia and S. Bobev, Acta Crystallogr. E **62**, i7 (2005).
[22] J. Rodriguez-Carvajal, Physica **192**, 55 (1993).
[23] C. Dallera, M. Grioni, A. Shukla, G. Vanko, J. L. Sarrao, J. P. Rueff, and D. L. Cox, Phys. Rev. Lett. **88**, 196403 (2002).
[24] K. Kummer *et al.*, Phys. Rev. B **84**, 245114 (2011).
[25] H. Yamaoka *et al.*, Phys. Rev. B **87**, 205120 (2013).
[26] Y. C. Tseng, D. Paudyal, Y. Mudryk, V. K. Pecharsky, K. A. Gschneidner, Jr., and D. Haskel, Phys. Rev. B **88**, 054428 (2013).
[27] C. Dallera, E. Annese, J.-P. Rueff, A. Palenzona, G. Vankó, L. Braicovich, A. Shukla, and M. Grioni, Phys. Rev. B **68**, 245114 (2003).
[28] G. Venturini, R. Welter, B. Malaman, and E. Ressouche, J. Alloys Compd. **200**, 51 (1993).
[29] F. Canepa, R. Duraj, C. Lefèvre, B. Malaman, A. Mar, T. Mazet, M. Napoletano, A. Szytula, J. Tobola, G. Venturini, and A. Vernière, J. Alloys Compd. **383**, 10 (2004).

[30] T. Mazet, O. Isnard, and B. Malaman, J. Phys.: Condens. Matter **17**, 1547 (2005).
[31] T. Mazet, H. Ihou-Mouko, and B. Malaman, J. Appl. Phys. **103**, 043903 (2008).
[32] T. Mazet, J. Tobola, G. Venturini, and B. Malaman, Phys. Rev. B **65**, 104406 (2002).
[33] N. E. Bickers, D. L. Cox, and J. W. Wilkins, Phys. Rev. B **36**, 2036 (1987).
[34] T. A. Costi, Phys. Rev. Lett. **85**, 1504 (2000).
[35] J. J. Parks *et al.*, Science **328**, 1370 (2010).
[36] R. Zitko, R. Peters, and Th. Pruschke, New J. Phys. **11**, 053003 (2009).
[37] K. Yoshimura, T. Nitta, M. Mekata, T. Shimizu, T. Sakakibara, T. Goto, and G. Kido, Phys. Rev. Lett. **60**, 851 (1988).
[38] T. Mazet, J. Tobola, and B. Malaman, Eur. Phys. J. B **34**, 131 (2003).
[39] H. Yamaoka, I. Jarrige, N. Tsujii, J.-F. Lin, N. Hiraoka, H. Ishii, and K.-D. Tsuei, Phys. Rev. B **82**, 035111 (2010).
[40] H. Sato *et al.*, Phys. Rev. B **89**, 045112 (2014).
[41] S. K. Malik, G. K. Shenoy, S. K. Dhar, P. L. Paulose, and R. Vijayaraghavan, Phys. Rev. B **34**, 8196 (1986).
[42] W. M. Temmerman, Z. Szotek, A. Svane, P. Strange, H. Winter, A. Delin, B. Johansson, O. Eriksson, L. Fast, and J. M. Wills, Phys. Rev. Lett. **83**, 3900 (1999).
[43] A. Svane, W. M. Temmerman, Z. Szotek, L. Petit, P. Strange, and H. Winter, Phys. Rev. B **62**, 13394 (2000).
[44] H. Winkelmann, M. M. Abd-Elmeguid, H. Micklitz, J. P. Sanchez, P. Vulliet, K. Alami-Yadri, and D. Jaccard, Phys. Rev. B **60**, 3324 (1999).
[45] D. Braithwaite, A. Fernandez-Pañella, E. Colombier, B. Salce, G. Knebel, G. Lapertot, V. Balédent, J.-P. Rueff, L. Paolasini, R. Verbeni, and J. Flouquet, J. Supercond. New Magn. **26**, 1775 (2013).